# An experimental study of the mixing of CO 2 and N 2 under conditions found at the surface of Venus

Sébastien Lebonnois, Gerald Schubert, Tibor Kremic, Leah Nakley, Kyle Phillips, Josette Bellan, Daniel Cordier

# An experimental study of the mixing of $CO_2$ and $N_2$ under conditions found at the surface of Venus

Sébastien Lebonnois [a,*], Gerald Schubert [b], Tibor Kremic [c], Leah M. Nakley [c], Kyle G. Phillips [d], Josette Bellan [e], Daniel Cordier [f]

[a] Laboratoire de Météorologie Dynamique (LMD/IPSL), Sorbonne Université, ENS, PSL Research University, Ecole Polytechnique, Institut Polytechnique de Paris, CNRS, Paris, France
[b] Department of Earth, Planet. and Space Sci., UCLA, CA, USA
[c] NASA Glenn Research Center, Cleveland, OH, USA
[d] HX5 Sierra, LLC, NASA GRC, Cleveland, OH, USA
[e] Jet Propulsion Laboratory, California Institute of Technology, Pasadena, CA, USA
[f] Groupe de Spectrométrie Moléculaire et Atmosphérique - UMR CNRS 7331, Campus Moulin de la Housse - BP 1039, Université de Reims Champagne-Ardenne, 51687 Reims, France

A B S T R A C T

Based on the only reliable temperature profile available in the deepest ∼10 km layer above Venus' surface (obtained by the VeGa-2 landing probe), the mixing conditions of the main constituents of Venus's atmosphere, $CO_2$ and $N_2$, have been questioned. In this work, we report the results of a series of experiments that were done in the GEER facility at Glenn Research Center to investigate the homogeneity of $CO_2/N_2$ gas mixtures at 100 bars and temperatures ranging from ∼296 K to ∼735 K. When the gas mixtures are initially well-mixed, separation of the two gases based on their molecular mass does not occur over the time scales observed; although, small systematic variations in composition remain to be fully interpreted. However, when $N_2$ is injected on top of $CO_2$ (layered fill), the very large density ratio makes it more difficult to mix the two chemical species. Timescales of mixing are of the order of $10^2$ hours over the height of the test vessel (roughly 60 cm), and even longer when the gas mixture is at rest and only molecular diffusion is occurring. At room temperature, close to the critical point of the mixture, large pressure variations are obtained for the layered fill, as $N_2$ slowly mixes into $CO_2$. This can be explained by large density variations induced by the mixing. For conditions relevant to the near-surface atmosphere of Venus, separation of $CO_2$ and $N_2$ based on their molecular mass and due to physical properties of the gas mixture is not demonstrated, but cannot be firmly excluded either. This suggests that if the compositional vertical gradient deduced from the VeGa-2 temperature profile is to be trusted, it would most probably be due to some extrinsic processes (not related to gas properties, e.g. $CO_2$ volcanic inputs) and large mixing time constants.

## 1. Introduction

Many properties of the deep atmosphere of Venus, between the surface and 10 km of altitude, are unknown. The Venus International Reference Atmosphere (VIRA, Kliore et al., 1985) suggests that in this region, the temperature increases from roughly 650 K to 735 K at the surface, while the pressure increases from ∼45 bar to 92 bar at the surface (Seiff et al., 1985). However, this model was built on data form the Pioneer Venus probes only down to 12 km (altitude at which the instruments stopped recording the temperatures), and extrapolated based on an adiabatic profile below this altitude. The VIRA model recommends an average mixture of 96.5% $CO_2$ and 3.5% $N_2$ as the

dominant gases (von Zahn and Moroz, 1985). However, these characteristics are based on very few in-situ data. Since questions were raised by Lebonnois and Schubert (2017) about the conditions of mixing in this region, the goal of the present work is to investigate experimentally the possibility that an intrinsic process might alter the vertical mixing of the two main constituents, that would be fast enough to counter the stirring due to large-scale dynamics. The interface region between the surface and the atmosphere, that includes the planetary boundary layer (Lebonnois et al., 2018), controls how angular momentum, energy and compounds are exchanged between the atmosphere and the surface of the planet. A good understanding of the mixing processes in this
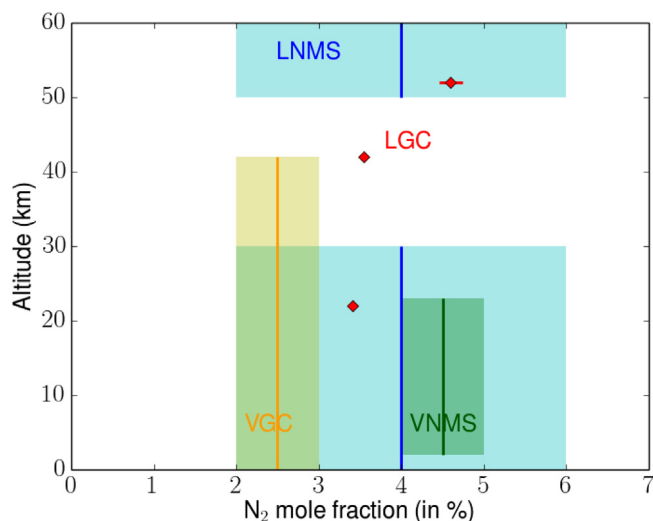
---

**Fig. 1.** Measurements of $N_2$ mole fraction in the atmosphere of Venus by the Pioneer Venus sounder probe (LGC (Oyama et al., 1980) and LNMS (Hoffman et al., 1980a)) and Venera 11 and 12 probes (VGC (Gelman et al., 1979) and VNMS (Istomin et al., 1979)). The LNMS measurements were blocked between 50 and 30 km by sulfuric acid coating of the MS leaks, and the published analysis only gives one global value, $4 \pm 2\%$ (Hoffman et al., 1980a).

region is therefore of high importance, particularly in the case of Venus, the atmosphere of which is characterized by a peculiar circulation, the superrotation (the entire atmosphere rotates much faster than the surface).

The only available and reliable temperature profile reaching to the surface of Venus was acquired by the VeGa-2 lander (Linkin et al., 1986; Zasova et al., 2006; Lorenz et al., 2018). Though this profile is in agreement with other in-situ temperature profiles measured by the Pioneer Venus probes above 12 km, it is a unique dataset below this altitude. The temperature profile displays a very peculiar feature below 7 km: it becomes highly unstable down to the surface (Seiff and the VEGA Balloon Science Team, 1987; Zasova et al., 2006). In a recent work, Lebonnois and Schubert (2017) interpreted this profile as the possible signature of a compositional gradient in this region, with the amount of nitrogen decreasing linearly with altitude from 3.5% above 7 km to zero at the surface. The mole fraction of nitrogen was measured by several mass spectrometers and gas chromatographs on-board the Pioneer-Venus Sounder probe (Hoffman et al., 1980a; Oyama et al., 1980) and the Venera 11 and 12 landers (Istomin et al., 1979; Gelman et al., 1979), in the altitude range from the surface to 60 km, depending on the instrument (see Table 2 in Hoffman et al., 1980b). Measured mole fractions of $N_2$ range from 2.5 to 4.5%, with an average value of 3.5%, as shown in Fig. 1. Some values correspond to similar altitude ranges, but are not compatible with each other. It is difficult to know if the dispersion in the measured values is due to instrumental problems or to local variations in the nitrogen abundance. The most accurate measurements are from the LGC measurements on-board Pioneer-Venus Large probe (Oyama et al., 1980), which indicate some difference between the nitrogen mixing ratio below and within the clouds. This gradient between 3.5% below the clouds and 4.6% at 52 km appears to be confirmed by the report of a nitrogen mixing ratio of 5.4% near 64 km, from the MESSENGER Neutron Spectrometer (Peplowski and Lawrence, 2016). The reason for this gradient and if it is related to the near-surface problem remains an open question. There were also measurements of the gas composition by gas chromatography onboard the Venera 13 and 14 landers, but the mole fraction of $N_2$ was not measured (Mukhin et al., 1983). No additional measurements of $N_2$ mole fraction in the atmosphere of Venus are reported in the literature.

The mixing of $CO_2$ and $N_2$ under pressures relevant to Venus's deep atmosphere was studied in one previous experiment. Hendry et al.

**Table 1**
Critical pressure and temperature for different mixtures of $CO_2$ and $N_2$.

|  | Pure $CO_2$ | 97% $CO_2$ 3% $N_2$ | 80% $CO_2$ 20% $N_2$ | 50% $CO_2$ 50% $N_2$ |
|---|---|---|---|---|
| Critical pressure (bars) | 73.8 | 85.9 | 103.6 | 98. |
| Critical temperature (K) | 304.1 | 301.9 | 284.3 | 264. |

(2013) investigated the mixing of a mixture of 50% $CO_2$ and 50% $N_2$ in mole fractions, at room temperature (296 K) and pressures 100 bar and higher. The experimental vessel was 18 cm in height, 8.7 cm in diameter. Composition was measured by gas chromatography from four different positions in the vessel: from the top, from the bottom, and from two intermediate positions. At 100 bar, the authors claimed that a stable composition was reached, with around 70% $N_2$ at the top, and around 90% $CO_2$ at the bottom. The vertical gradient in composition was even higher at higher pressures. No detailed explanation was given for the mechanism that could justify such a vertical compositional gradient, though density-driven separation through natural convection was mentioned. Despite the different temperature and mixing ratio conditions, the vertical gradient measured in this gas mixture was a good indication that such a mechanism, that remained to be understood, could be at play in the deep atmosphere of Venus (Lebonnois and Schubert, 2017).

In order to better understand the behavior of the mixtures of $CO_2$ and $N_2$ in temperature and pressure conditions similar to the deep atmosphere of Venus, we designed an experiment using the Glenn Extreme Environment Rig (GEER) facility at NASA Glenn Research Center, to monitor the composition in a vessel similar to the one used in the Hendry et al. (2013) experiment, though taller. Conditions in the vessel were varied step by step from their experimental conditions to Venus's deep atmospheric conditions, measuring the vertical gradient in composition. The critical points of $CO_2$ as well as different mixtures of $CO_2$ and $N_2$ are indicated in Table 1. Morellina and Bellan (2019) calculated the spinodal (which contains all of the critical points) of the CO2/N2 mixture and showed that the lower Venus atmosphere thermodynamic conditions place it in the single-phase, supercritical regime for this mixture. In the Hendry et al. (2013) experimental conditions, the mixture is close to the critical point, but in near-surface Venus conditions, the high temperatures indicate that the density conditions, although supercritical, are much closer to perfect gas conditions. Though the dynamical conditions in the laboratory experiments are different from the atmosphere of Venus in terms of turbulence and mixing, the goal of this work was to investigate the hypothesis of an intrinsic separation process (i.e. related to gas properties), fast enough to counter mixing in the near-surface layer of Venus's atmosphere. In Section 2, details are given on the experimental design and protocol. The experiment was carried out at NASA Glenn Research Center from August 8 to September 5, 2018. The results are analyzed in Section 3, with a concluding discussion in Section 4.

## 2. GEER experiment set-up and implementation

### 2.1. Hardware configuration

The Glenn Extreme Environment Rig (GEER) is a research facility capable of operating at conditions up to 810 K and 100 bar with nine or more chemical species. GEER is equipped with a 0.8 $m^3$ stainless steel pressure vessel, a fully automated gas mixing system, and real time gas analysis system. To best accommodate the number of experimental conditions selected for the experiment, a smaller, cylindrical pressure vessel was implemented to reduce the time needed to transition between experimental conditions. The smaller pressure vessel, referred to as the test vessel, was installed inside of the GEER pressure vessel in the vertical position, and fully integrated with the GEER process system.
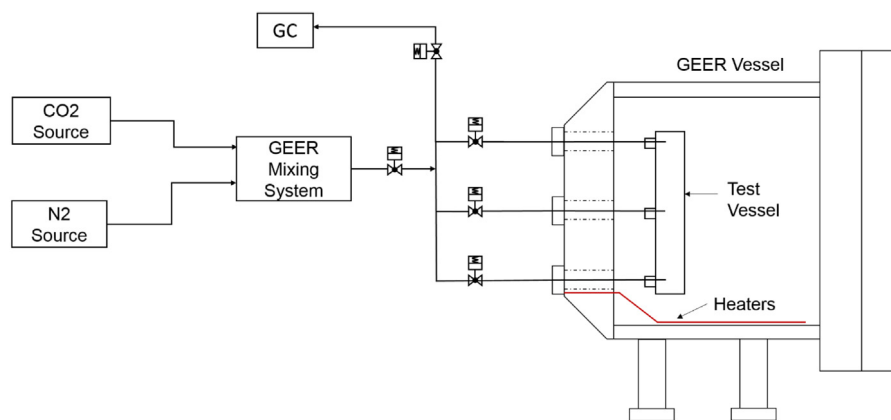
**Fig. 2.** Experimental set-up.

The test vessel was constructed out of stainless steel (to be more precise, 304 stainless steel) and included three gas sampling ports along the vertical side wall. The ports were used to collect gas samples from the top, middle, and bottom of the test vessel. The overall length of the test vessel was 70 cm with an internal diameter measuring 8.7 cm and internal volume of 3966 cm$^3$. Fig. 2 shows the GEER system as configured for the experiment.

The gas sampling ports were constructed of heavy wall stainless steel tube that extended outside of the GEER vessel. Each port was equipped with an isolation valve to allow for independent control and sampling. A thermocouple was inserted through each port, into the vessel center, to measure the local gas temperature at the top, middle, and bottom. Pressure sensors were installed on the external sections of the middle and bottom sampling ports just before the isolation valves. A common manifold directed gas to and from the test vessel, and to the gas chromatograph (GC) for analysis.

Gas samples were analyzed by an Inficon MicroGC Fusion with an accuracy specification of $\pm 10\%$ and relative standard deviation of $< 1\%$. The GC was calibrated with five certified gas mixtures in addition to pure $CO_2$ and pure $N_2$. The five mixtures contained 30% $CO_2$ and 70% $N_2$, 50% $CO_2$ and 50% $N_2$, 70% $CO_2$ and 30% $N_2$, 90% $CO_2$ and 10% $N_2$, and 97% $CO_2$ and 3% $N_2$.

### 2.2. Experimental conditions

At the start of each experiment, the test vessel was first evacuated to remove residual gas and then preheated to a specified temperature. Next, the various gas mixtures were delivered to the test vessel using a high pressure gas booster pump. Once the pressure reached 100 bar at the specified temperature, gas samples were collected from the top, middle, and bottom of the test vessel. The sample manifold and process lines to the GC were evacuated after every sample.

Two different methods were used to blend and deliver gas to the test vessel. For the first method, premixed gas was blended in a 57 L receiver tank and then transferred to the test vessel as a single, premixed fluid. This method was selected to ensure that $CO_2$ and $N_2$ were adequately mixed before delivery to the test vessel. Samples were drawn from the receiver and analyzed by GC to verify composition before transfer to the test vessel. For the second method, gas mixtures were blended directly inside of the test vessel. Unless otherwise stated, $CO_2$ was added first followed by $N_2$. The gas mixing method used in each experiment is listed in Table 2.

The experimental conditions, referred to as levels, were separated into two phases. Phase 1 studied various mixtures at low temperature. Phase 2 investigated the effects of temperature on mixtures of constant molar ratio. The final two levels in phase 2 were conducted at high temperature with adjustments made to the gas composition. Table 2 includes a complete list of the experimental conditions. The different names we used for the experiments are explained in the next Section.

**Table 2**
Performed experimental conditions.

| Phase | Level | Temperature | Pressure | Mole fractions | | Gas mixture[a] | Duration |
|---|---|---|---|---|---|---|---|
| | | (K) | (bar) | $CO_2$ (%) | $N_2$ (%) | | (h) |
| | P1L0 | 296 | 100 | 50 | 50 | Premixed | 22 |
| | P1L0H | 296 | 100 | 50 | 50 | Layered | 120 |
| | P1L1H | 310 | 100 | 50 | 50 | Layered | 3 |
| Phase 1 | P1L2 | 310 | 100 | 80 | 20 | Premixed | 28 |
| | P1L2H | 310 | 100 | 80 | 20 | Layered | 26 |
| | P1L4 | 310 | 100 | 97 | 3 | Premixed | 16 |
| | P1L4H | 310 | 100 | 97 | 3 | Layered | 24 |
| | P2L5 | 500 | 100 | 97 | 3 | Premixed | 64 |
| | P2L5H | 500 | 100 | 97 | 3 | Layered | 26 |
| | P2L5H2 | 500 | 100 | 97 | 3 | Layered | 22 |
| Phase 2 | P2L10 | 735 | 100 | 97 | 3 | Premixed | 57 |
| | P2L10P | 735 | 100 | 97 | 3 | Layered[b] | 115 |
| | P2L11H | 735 | 100 | 90 | 10 | Layered | 46 |
| | P2L12H | 735 | 100 | 95 | 5 | Layered[c] | 120 |

[a]Layered means $CO_2$ was introduced first, then $N_2$, from the top port, unless stated otherwise.
[b]$CO_2$ was injected from the bottom port into the premixed gas mixture.
[c]$N_2$ was introduced first, then $CO_2$ was introduced from the bottom port.

### 2.3. Experimental strategy

In their experiment, Hendry et al. (2013) stated that with a mixture of 50% $N_2$ / 50% $CO_2$ (in mole fractions) at 296 K and 100 bar, there was a stable vertical gradient in composition. Based on this, our strategy was first to reproduce this experiment, then to measure the potential vertical gradient in composition in various conditions, for different mole fractions of $N_2$ (phase 1) before increasing the temperature for a Venus-like mixture, up to 735 K (phase 2).

Our first experiment (P1L0) used a 50% $N_2$ / 50% $CO_2$ mixture, premixed at low pressure (in the receiver tank), under the same conditions as the Hendry et al. (2013) experiment. As will be shown in Section 3, no large vertical gradient in composition was observed in this experiment. Therefore, our strategy was modified. Since the protocol described in Hendry et al. (2013) mentioned that they filled $CO_2$ first, then $N_2$, the same protocol was adopted. In addition to using the premixed gas mixture, the same masses of $CO_2$ and $N_2$ were introduced in the test vessel, one after the other (these experiments are labeled with an "H" in their code). The evolution of the composition at the three ports was then monitored over timescales of one day to several days, durations that were not yet long enough for molecular diffusion timescales but were limited by the total time allocated to our experiments. Because of this limited time, only a few experimental conditions were investigated (hence the limited level values, see Table 2). In Phase 1, P1L0 and P1L0H were carried out at 296 K. Then at 310 K, the mixtures were 50% $N_2$ / 50% $CO_2$ (P1L1H), 20% $N_2$ / 80% $CO_2$ (P1L2,
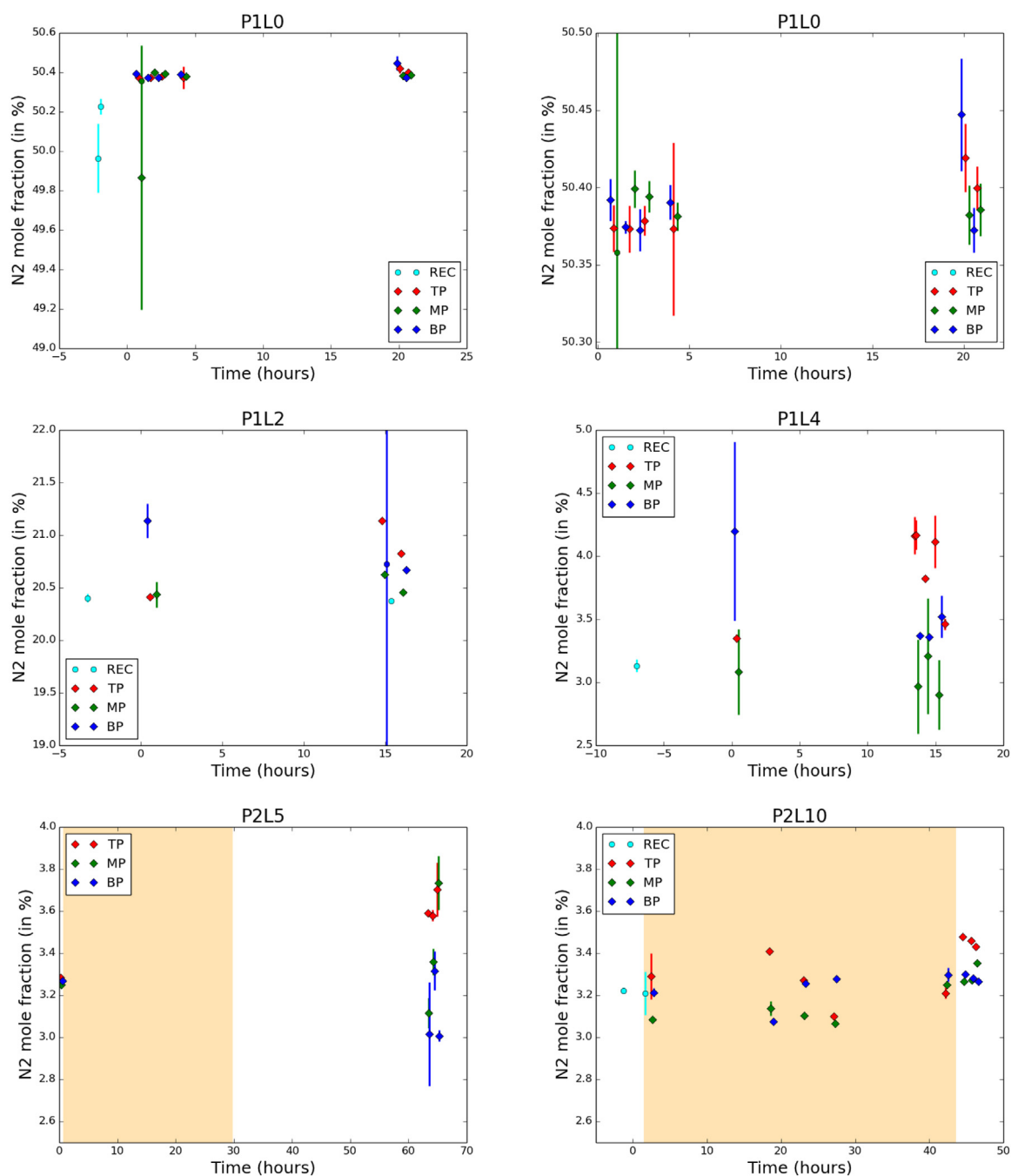
**Fig. 3.** $N_2$ mole fractions in the premixed experiments. Each sample is plotted with a diamond symbol, with the standard deviation over the ensemble of analyses shown with vertical lines. When correction was needed, a circular symbol is plotted with the corrected value. Red is used for the top port samples (TP), green for middle port samples (MP) and blue for bottom port samples (BP). Cyan is used for samples taken from the premix receiver. Time is indicated in hours after the start of each experiment (end of the filling phase). Heating phases are indicated with orange areas. Conditions for each experiment (compositions in mole fraction; all experiments are at 100 bar, except during the heating periods where the pressure raises with temperature, to reach 100 bar at the expected temperature): P1L0 = 50% $CO_2$ / 50% $N_2$, 296 K (2 panels, to zoom on the 50.3–50.5 values); P1L2 = 80% $CO_2$ / 20% $N_2$, 310 K; P1L4 = 97% $CO_2$ / 3% $N_2$, 310 K; P2L5 = 97% $CO_2$ / 3% $N_2$, 500 K; P2L10 = 97% $CO_2$ / 3% $N_2$, 735 K.

P1L2H) and 3% $N_2$ / 97% $CO_2$ (P1L4, P1L4H). In Phase 2, with a 3% $N_2$ / 97% $CO_2$ mixture, we increased the temperature first to 500 K (P2L5, P2L5H2 — there was a problem with experiment P2L5H, which was entirely discarded and redone), then to 735 K (P2L10, P2L10P, P2L11H, P2L12H).

At 735 K, after the P2L10 experiment, it was decided to investigate the behavior in the test vessel when a "plume" of $CO_2$ was injected from the bottom (experiment P2L10P). For the last layered experiments, the protocol was slightly modified: for P2L11H, $CO_2$ was injected first, then $N_2$ from the top port, in 10% $N_2$ / 90% $CO_2$ proportions; for P2L12H,

$N_2$ was inserted first in the test vessel, then $CO_2$ was added from the bottom port, in 5% $N_2$ / 95% $CO_2$ proportions.

## 3. Analysis of the results

Each sample was analyzed five times by the gas chromatograph (GC). Each of these analyses gives the mole fractions of $N_2$ and $CO_2$. The average mole fraction for $N_2$ is the result reported in our plots for each sample, and the standard deviation among the five analyses gives the uncertainty associated with this result. In some cases, a detailed
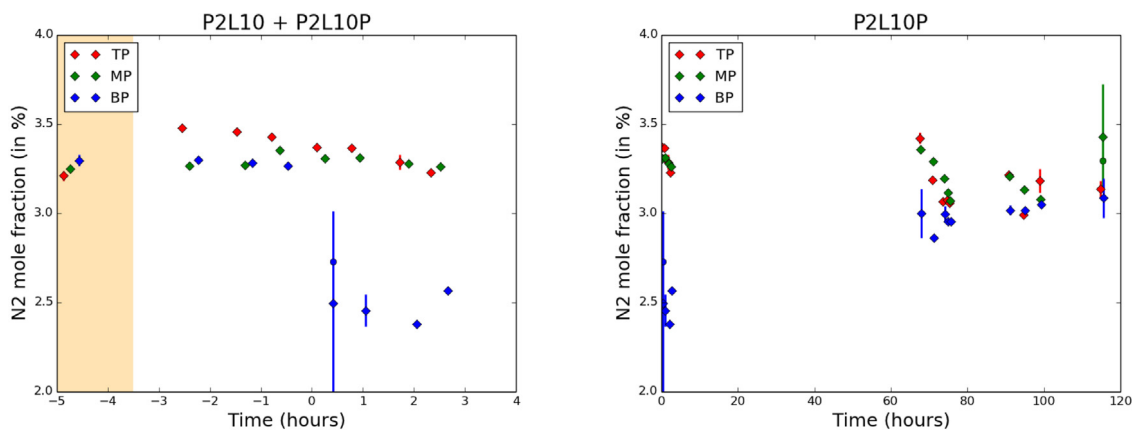
**Fig. 4.** (left) Last samples for the P2L10 experiment (see Fig. 3), followed by the first samples of the P2L10P experiment. The origin of the time axis corresponds to the end of the additional $CO_2$ injection from the bottom port. (right) Complete P2L10P experiment. Symbols and colors are similar to Fig. 3.

evaluation of the five analyses indicates a clear anomaly in one (or several) of the analyses. In these cases, a corrected value is computed by averaging, after removing the anomalous measurement(s). This corrected value is also indicated on the figures. In a few cases a complete sample was discarded and redone. These discarded samples are not plotted on the figures.

### 3.1. Premixed gas mixtures

Fig. 3 shows the evolution with time of the mole fraction of $N_2$ measured at each of the ports, for all the experiments done with a premixed gas mixture (see Table 2). In all the panels of Fig. 3, points tend to be grouped together near the average value. P1L0 does not show dispersion (mostly within $\pm0.03\%$ around average). For P2L10 (Venus temperature and pressure conditions), the dispersion is small ($\pm0.3\%$ around average), with no clear trend. Heating occurred during the experiment and may have affected the turbulence within the test vessel. However, in the hours after heating, the $N_2$ mole fractions at the top port are systematically slightly higher than at the other ports.

For P1L2, P1L4 and P2L5, a consistent behavior may be seen for the evolutions of the top port (TP) and bottom port (BP) $N_2$ mole fractions. In P1L2 and P1L4, the TP $N_2$ mole fraction is raised by $\sim 0.6\%$ in approximately 15 h, while the BP $N_2$ mole fraction, which started higher than at the other ports, goes down by approximately the same amount. The middle port (MP) $N_2$ mole fraction is close to the receiver value, and does not evolve much.

In P2L5, some overfill occurred prior to the heating phase. Adjustment was done by venting some gas from the test vessel. This may have induced turbulence, which may explain why the three ports are almost exactly at the same composition for the first samples. This composition is consistent with the receiver points measured later, on Aug. 22, before P2L10. Then, $N_2$ mole fractions at TP and BP evolved as in the P1L2 and P1L4 experiments, but with a much slower rate ($\sim 0.3\%$ in 60 h).

In P2L10, while raising the temperature from 500 to 735 K, the composition does not seem to have evolved in a consistent way, remaining close ($\pm0.2\%$) to the premixed composition measured in the receiver tank. However, the $N_2$ mole fractions at TP tend to be slightly higher than at the other ports at the end of the experiment, as in the previous cases.

### 3.2. Plume experiment

For this experiment, some gas was vented from the test vessel after the P2L10 experiment, with the pressure decreasing from ~95 to ~85 bar, then pure $CO_2$ was injected from the bottom port to reach roughly 100 bar. The time evolution of the $N_2$ mole fractions is shown in Fig. 4.

At the top port, the small difference with the MP mole fraction present at the end of P2L10 tends to shrink. During the P2L10P experiment, TP and MP abundances are similar. At the bottom port, the mole fraction of $N_2$ was down to 2.5% after $CO_2$ injection. This value may be surprising as we had injected pure $CO_2$ from the bottom port and might be expecting less $N_2$. One hypothesis is that due to the position of the bottom port (a couple of centimeters above the bottom of the vessel), the lower part of the test vessel was well mixed, therefore maintaining some $N_2$ present at BP. It seems difficult to avoid turbulent mixing, though future research on the topic may consider mitigating this mixing through the design of the test apparatus and process system. Turbulent mixing of a turbulent plume of $N_2$ injected into quiescent $CO_2$ has been simulated by Gnanaskandan and Bellan (2018) using Direct Numerical Simulations and it has been shown that formation of side-jets improves mixing, which otherwise, if left to molecular processes alone, is a very slow process at high pressures. In the overall test vessel, the mixing (diffusion and/or turbulence) brings everything back to well mixed after ~100 h.

### 3.3. Layered fills

#### 3.3.1. Composition evolution

Figs. 5 and 6 show that filling $N_2$ after $CO_2$ results in a clearly unmixed state. At low temperature (Fig. 5) and high $N_2$ content, the initial pressure is lower than the pressure of the premixed state (80 bars at the beginning of P1L0H). As illustrated in Fig. 7, pressure gradually increases as $N_2$ mixes into $CO_2$. This behavior is analyzed in the next subsection.

P1L0H is the closest to the experimental protocol indicated in Hendry et al. (2013). However, it is difficult to understand their results and their protocol from the observations that were made during our experiments. According to those authors, the situation was stable for "several hours". It is clearly visible in Fig. 5 that under these conditions, the composition evolves on timescales of several days, so the state they observed may have been an unsteady but very slowly evolving state. Filling $CO_2$ first, then $N_2$, it is also difficult to understand how they could assure an equimolar mixture and reach a pressure of 100 bar (the pressure indicated in their experiment), given that the heterogeneity they measured in their test vessel must have strongly affected the pressure.

In all these experiments, the variations of the $N_2$ mole fractions at each port indicate mixing over timescales of several tens of hours. The mixing timescales are changing within each experiment: timescales observed when the system is not perturbed (during nights and weekends) are much longer than when there is sampling. Sampling seems to accelerate the mixing, possibly by inducing additional processes. These processes may be small-scale turbulence (Gnanaskandan and Bellan,
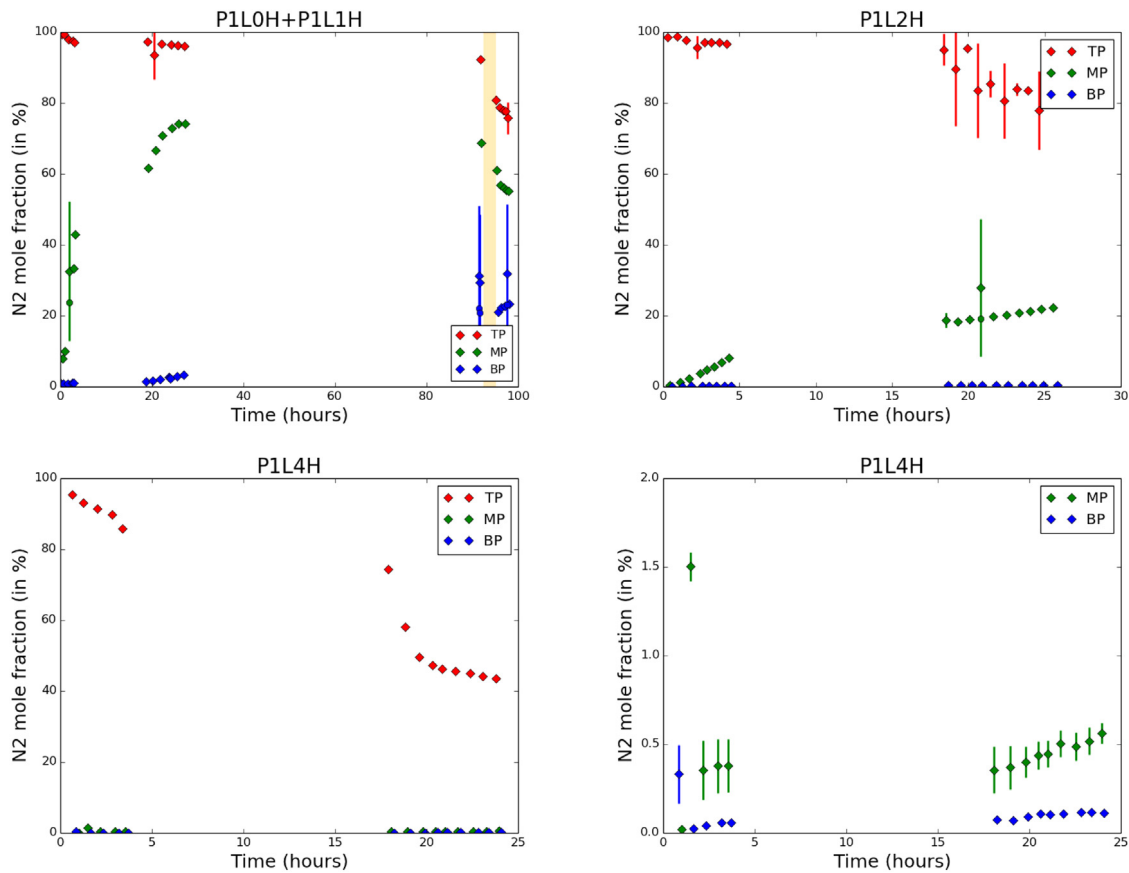
**Fig. 5.** Layered experiments at 296 K (P1L0H) and 310 K (P1L1H, P1L2H, P1L4H). Symbols and colors are similar to Fig. 3. Average conditions for each experiment (all experiments are at 100 bar): P1L0H = 50% $CO_2$ / 50% $N_2$, 296 K; P1L1H = 50% $CO_2$ / 50% $N_2$, 310 K; P1L2H = 80% $CO_2$ / 20% $N_2$, 310 K; P1L4H = 97% $CO_2$ / 3% $N_2$, 310 K (2 panels, to zoom on the 0.-2. values).

2018), or some circulation patterns within the vessel, though it is not possible to determine their nature with our experimental set-up. Molecular diffusion coefficients are estimated to be of the order of 2-8×10$^{-7}$ m$^2$/s (depending on temperature) (Haynes, 2014), which give timescales for diffusion over 30 cm around 1-5×10$^5$ s, i.e. 30–140 h. This is compatible with our observed evolutions (when the system is left unperturbed).

Some peculiar behaviors should be noted:

- P2L5H2: between $t = 16$ h to $t = 19$ h, the BP $N_2$ mole fraction is higher than the MP $N_2$ mole fraction. It reverses near $t = 20$ h.
- P2L11H: MP $N_2$ mole fraction is 2%–3% lower than BP after $t = 20$ h, even though the TP $N_2$ mole fraction converges towards the BP mole fraction.
- P2L12H: The reverse is true in this case, when $CO_2$ was filled through the bottom port. MP $N_2$ mole fraction is now higher than both TP and BP mole fractions after convergence.

A hypothesis to explain these last two observations is that there might be an internal circulation pattern that results in isolation of the middle port, yielding a value less rich in $N_2$ than average in P2L11H and more rich than average in P2L12H.

### 3.3.2. Distribution of nitrogen and pressure evolution

The variations of pressure observed during experiments P1L0H and P1L2H (Fig. 7) are due to the variation of the density of the gas mixture depending on the mole fraction of $N_2$. This is due to strong non-ideal effects, as the system is close to the critical point. In this Section, this peculiar behavior is analyzed in more detail.

If the masses of $N_2$ and $CO_2$ introduced in the cell are respectively $m_{N_2}$ and $m_{CO_2}$, while the cell is at a fixed temperature $T_0$, then the pressure $P_{ini}$ in the initial state of the system, described by a distribution of $N_2$ mole fraction $x(h)$ as a function of height $h$ in the test vessel, is given by

$$\int_{h=0}^{H} \rho(x(h), P_{ini}, T_0)\, A\, dh = m_{N_2} + m_{CO_2} \qquad (1)$$

with $V_{tot} = A \times H$ the inner volume (m$^3$) of the cell, $A$ the surface of its base and $H$ its height, $\rho(x(h), P_{ini}, T_0)$ is the density (kg m$^{-3}$) of the gas mixture for a given $x$ at the relevant pressure and temperature conditions. The pressure $P_{fin}$ reached by the system under its final, fully mixed state with $N_2$ mole fraction $\overline{x}$ is ruled by

$$\rho(\overline{x}, P_{fin}, T_0)\, V_{tot} = m_{N_2} + m_{CO_2} \qquad (2)$$

where the density of the fully mixed fluid is $\rho(\overline{x}, P_{fin}, T_0)$. It is worth noting that, in the case where the fluid is regarded as an ideal gas, both equations lead to the same value for the pressure, which can be written

$$P_{ideal} = \frac{RT_0}{V_{tot}} \left( \frac{m_{N_2}}{M_{N_2}} + \frac{m_{CO_2}}{M_{CO_2}} \right) \qquad (3)$$

where $R$ is the gas constant, and $M_i$ the molar mass of compound $i$. For instance, in the case of the P1L2 experiment ($x = 0.20$, 310 K) the assumption of an ideal gas behavior leads to a pressure of $\sim 169$ bars, while the GEER measurement gives 100.0 bars for the final state. As we can see, neglecting the intermolecular interactions, *i.e.* the non-ideal effects, implies a clear over-estimation for the pressure, in addition to non-differentiated pressures between the initial and final state.

To evaluate the density in the system $\rho(x, P, T)$, we used two different equations of state (EoS). Duan et al. (1992a) introduced a generalization to the system $CH_4$-$CO_2$-$H_2O$, of the EoS originally proposed
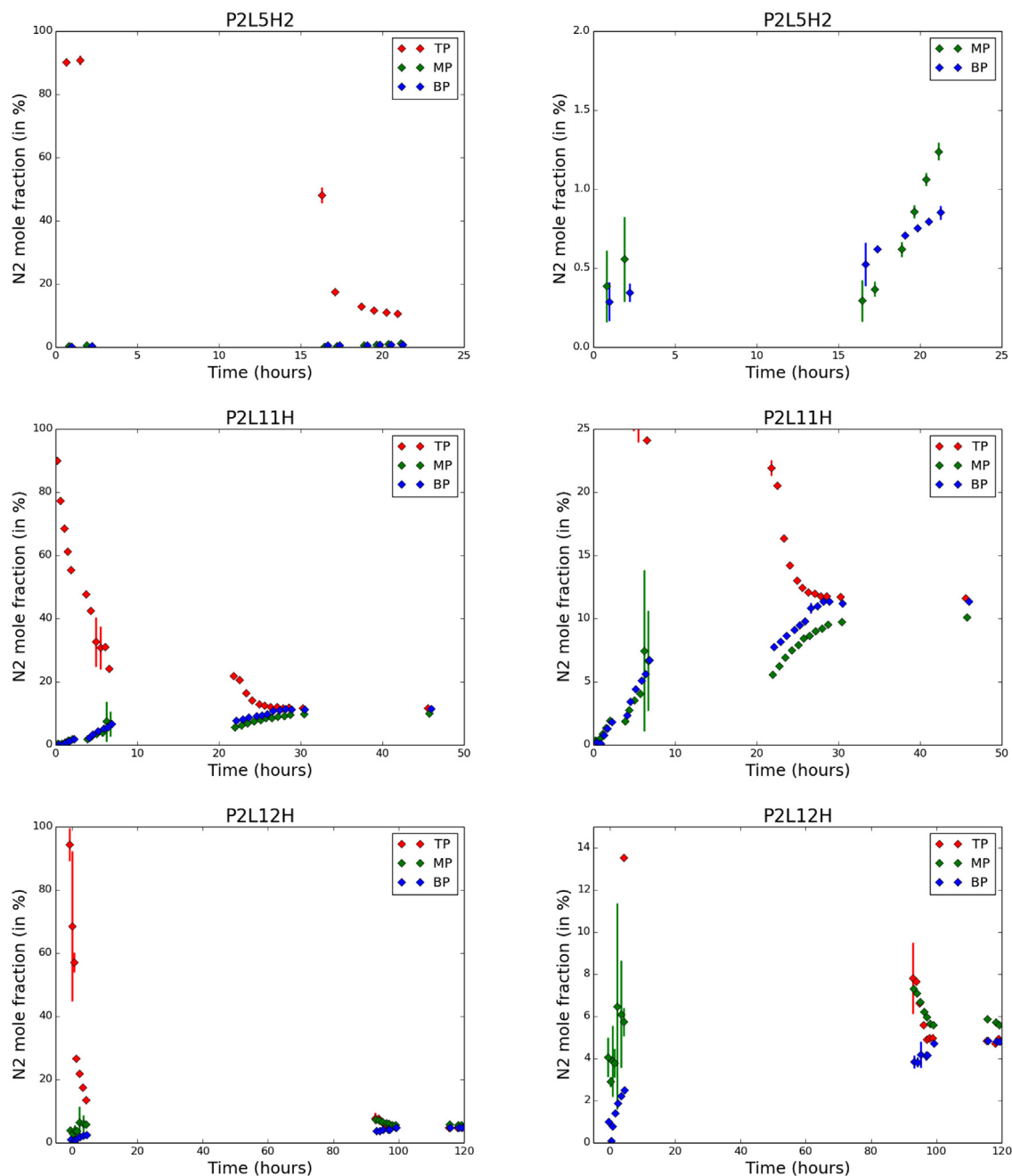
**Fig. 6.** Layered experiments at 500 K (P2L5H2) and 735 K (P2L11H and P2L12H). Right column is focused on lowest values of each experiment. Symbols and colors are similar to Fig. 3. Average conditions for each experiment (all experiments are at 100 bar): P2L5H2 = 97% $CO_2$ / 3% $N_2$, 500 K; P2L11H = 90% $CO_2$ / 10% $N_2$, 735 K; P2L12H = 95% $CO_2$ / 5% $N_2$, 735 K.

by Lee and Kesler (1975). In the context of geological fluids, Duan et al. (1992b) extended the validity of their EoS, in order to predict the $PVT$ supercritical properties of $CO_2$, $N_2$, CO, $H_2$, $O_2$ and $Cl_2$. Finally, this approach has been applied to supercritical fluids mixtures by Duan et al. (1996) (hereafter D96). However, for pure $CO_2$ (and therefore low values of $x$), densities computed with this EoS are in disagreement with the Span and Wagner (1996) EoS, dedicated to pure $CO_2$. Therefore, we used also another EoS called Perturbed-Chain Statistical Associating Fluid Theory (here-after: PC-SAFT, Gross and Sadowski, 2001) which is widely employed in the chemical engineering community. The PC-SAFT has been successfully introduced to the study of Titan by Tan et al. (2013, 2015), Luspay-Kuti et al. (2015) and Cordier et al. (2016). In the frame of PC-SAFT, molecules are considered as "chains" of segments where each molecule is characterized by its pure-component

parameters: the number of segment $m$, the segment diameter $\sigma$ (Å) and the segment energy of interaction $\epsilon/k_B$ (K). The PC-SAFT is extended to mixtures using the Berthelot–Lorentz combining rule for the dispersive energy, resulting in a single binary parameter $k_{ij}$. Our implementation of PC-SAFT consists of a set of FORTRAN 2008 object-oriented subroutines written from scratch. The PC-SAFT parameters $m$, $\sigma$ and $\epsilon/k_B$ have been taken in Gross and Sadowski (2001) in the case of carbon dioxide, and in the NIST database for nitrogen. The interspecies interaction parameter $k_{ij}$ has been set to zero. In Fig. 8, we have compared historical measurements (Haney and Bliss, 1944) of molar volume of $CO_2$-$N_2$ mixtures under supercritical conditions, with our implementation of these two different EoS. This is also the empirical data originally used by Duan et al. (1996). As we can see, the agreement between experiments and both approaches is rather good, as
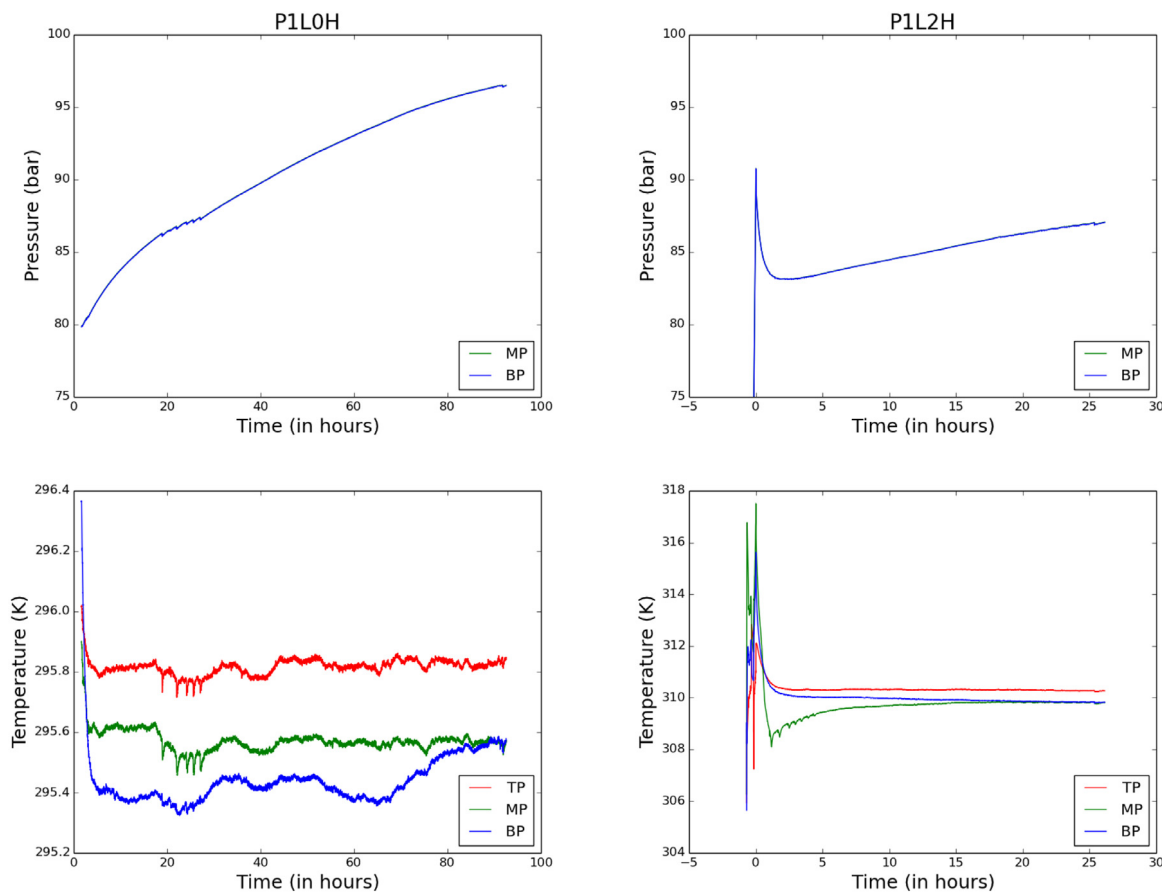
**Fig. 7.** Evolution of the pressure (upper row) and temperature (lower row) inside the test vessel during the P1L0H (left) and P1L2H (right) layered experiments.

**Table 3**
Consistency between measured mass and measured pressures in the P1L0 and P1L2 experiments.

| Level | Mass (kg) | Pressure (bar) | Mass[a] (kg) | Pressure[b] (bar) | Error[c] (%) |
|-------|-----------|----------------|--------------|-------------------|--------------|
|       | Measured  |                | Deduced      |                   |              |
| P1L0  | 0.756     | 100.2          | 0.726        | 103.7             | 4./3.5       |
| P1L2  | 1.07      | 100.0          | 0.934        | 109.5             | 7.5/9.1      |

[a] $P_{fin}$ is fixed to measurement in Eq. (2), total mass is computed (D96 EoS).
[b] Total mass is fixed to measurement in Eq. (2), $P_{fin}$ is computed (D96 EoS).
[c] error=200×(measured-deduced)/(measured+deduced); on mass/on pressure.

an example at 100 bar D96 gives 197 cm$^3$ mol$^{-1}$ while Haney and Bliss (1944) provide ∼ 195 cm$^3$ mol$^{-1}$. It should be emphasized that Haney and Bliss (1944) have "smoothed" their results, introducing some biases in their data. For the case where $x_{CO_2} \sim x_{N_2} \sim 0.50$ and $P = 100$ bar, the molar volume of the fully mixed fluid, present in the GEER test vessel, may be evaluated to ∼ 189 cm$^3$ mol$^{-1}$ (based on the measured mass).

For the mixed state, we can provide the mass of gas mixture introduced as it was measured during the experiment, and solve numerically Eq. (2) with a Newton–Raphson algorithm (see for instance Press et al., 1992) to deduce the final state pressure $P_{fin}$. We can also use the measured pressure and compute the total mass of gas mixture. These calculations are summarized in Table 3. For P1L0, we have a 4% error between the measured mass and the expected mass for the measured pressure. For P1L2, the error is worse, reaching 8%. When we started this experiment, some technical problems forced us to fill the test vessel in two different steps, which may have lead to a degraded estimation of the injected mass.

For the initial layered state, Eq. (1) may be used to infer some (limited) information on the vertical distribution of N$_2$ in the test vessel. Given the pressure $P_{ini}$, the temperature $T_0$, the PC-SAFT EoS and an assumed distribution of N$_2$ $x(h)$ as a function of height in the test vessel, the total masses of N$_2$ and CO$_2$ are computed with the following equations, similar to Eq. (1) for each component:

$$\int_{h=0}^{H} \rho(x(h), P_{ini}, T_0) x(h) \frac{M_{N_2}}{\mu(h)} A \, dh = m_{N_2} \tag{4}$$

$$\int_{h=0}^{H} \rho(x(h), P_{ini}, T_0)(1 - x(h)) \frac{M_{CO_2}}{\mu(h)} A \, dh = m_{CO_2} \tag{5}$$

where $\mu(h) = x(h) M_{N_2} + (1 - x(h)) M_{CO_2}$ is the mean molecular mass at height $h$. Fitting $m_{CO_2}$ and $m_{N_2}$ to the masses of CO$_2$ and N$_2$ initially inserted can be done by adjusting the profile $x(h)$. Of course, this is a very approximate method, potentially with multiple solutions, but we used it to demonstrate how the distribution of N$_2$ inside the test vessel affects the pressure (Fig. 9). An example of a distribution that fits the pressure, temperature, and composition at the ports obtained at the beginning of the P1L2H experiment is shown in Fig. 9b. For P1L0H, however, such a fit is impossible with the measured value of $x = 0.10$ at the middle port. Given the mass of N$_2$ introduced, assuming that most of it is still in the upper half of the test vessel is not sufficient (see Fig. 9a). Pressure and mass can be consistent only with N$_2$ dominating well below the middle port, while CO$_2$ is close to condensation at the bottom of the test vessel. One hypothesis to understand this problem is that the mixing of the two gases is so difficult that at the beginning of the experiment, strong inhomogeneities are still present in the test vessel, affecting the validity of our approach. Panels c and d of Fig. 9 illustrate how these two initial states might have evolved after 26 to 27 h.
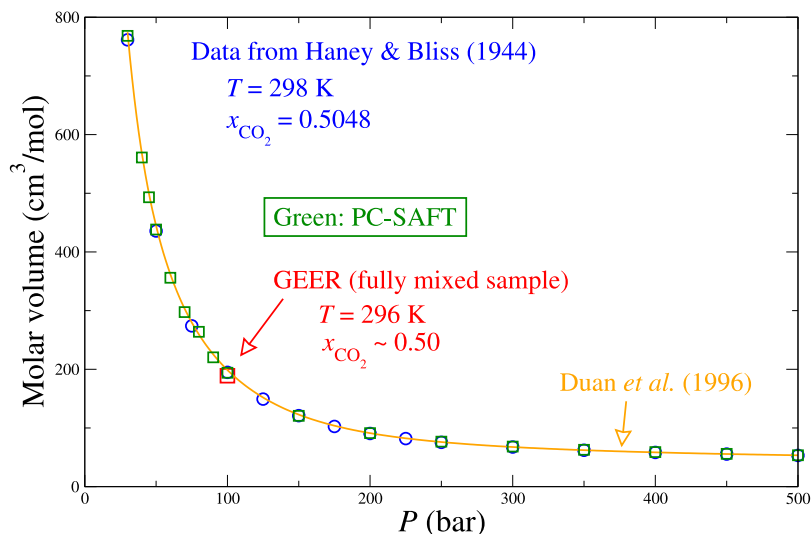
**Fig. 8.** A comparison between data from Haney and Bliss (1944) (blue circles), our implementation of the D96's EoS (orange solid line), the implementation of the PC-SAFT EoS (green squares), and one comparable data-point from GEER experiment (P1L0, red square).
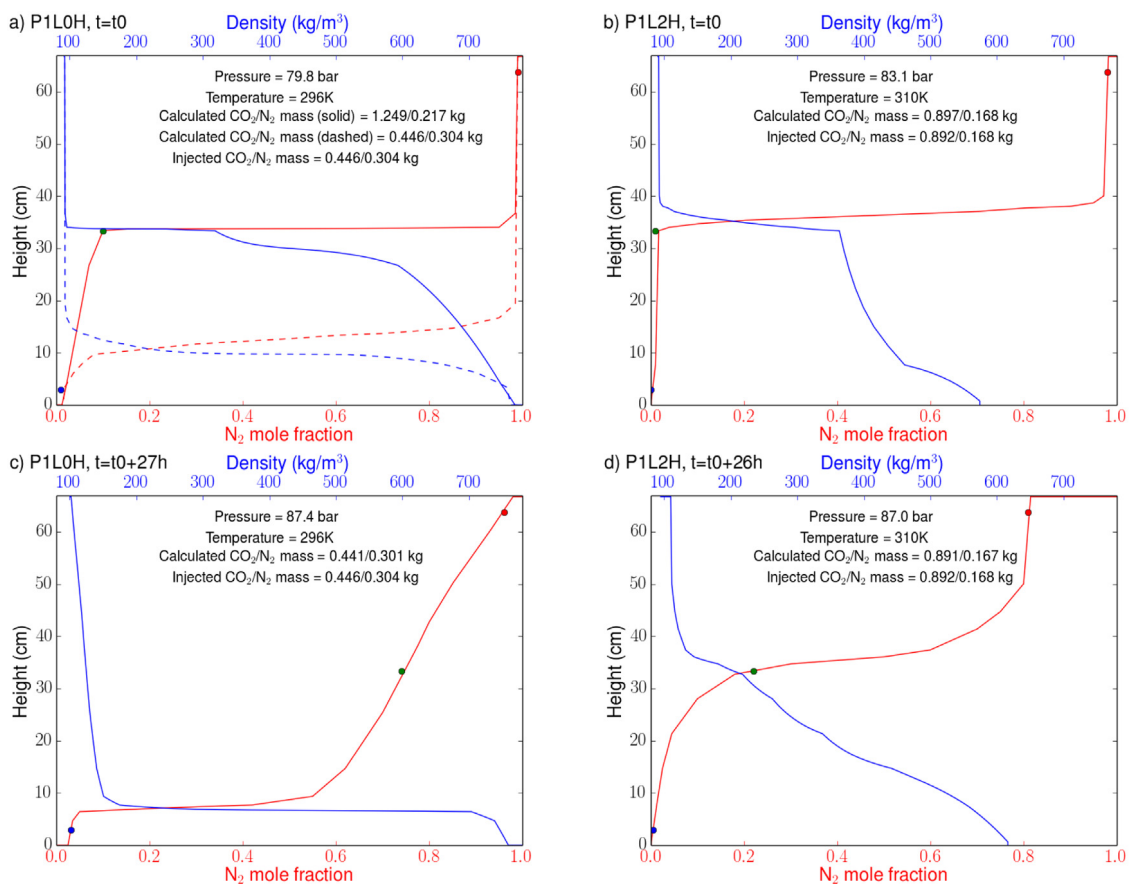


**Fig. 9.** Possible profiles of $N_2$ abundances within the test vessel, in order to fit the masses of $CO_2$ and $N_2$ initially introduced. (a) Initial state of the P1L0H experiment, with two different hypotheses: (solid) consistent with observed data points from our experiment or (dashed) consistent with the injected masses; (b) initial state of the P1L2H experiment; (c) P1L0H after 27 h; (d) P1L2H after 26 h. In blue, the profile of the density (computed with the PC-SAFT EoS) is shown. The composition measured in our experiment at the three ports are also plotted with circles (colors similar to Fig. 3–7).

## 4. Discussion

**Separation ?** In the premixed experiments, from P1L2 to P2L10, there seems to be a consistent pattern, with some limited redistribution of nitrogen preferentially toward the top of the test vessel. The clearest case is the P2L5 experiment. It remains very difficult to interpret such a behavior. There might be a macroscopic redistribution of $N_2$ within the test vessel: $N_2$ mole fraction fluctuations may not be erased by the very slow diffusion, so that density redistribution might be occurring. Our experiments are too limited for a firm conclusion, but our results clearly suggest that additional work is needed, both experimental and theoretical.

Designing a new experiment to investigate the possibility of such a redistribution of nitrogen would need to be thought carefully in order to measure variations in nitrogen content of the order of 0.1% (for an averaged mole fraction of 3 to 4%), in a very uniform and stable thermal environment. Measuring precisely the variations of composition in time over long periods, with the minimum of perturbations due to the measurements, would be needed to determine the timescale of the potential separation process.

**A difficult mixing.** While there is no clear-cut demonstration of separation, the experiments suggest that compositional gradients can last for long periods of time. Compositional variations within the test vessel may be mostly related to turbulent patterns, that are difficult to understand or monitor. This experimental study was not designed to measure the diffusion coefficients. However, the results of the layered experiments indicate that molecular diffusion processes are very slow, compatible with estimations of the molecular diffusion coefficients. Mixing is efficient mainly through turbulent or circulation processes. The study of Gnanaskandan and Bellan (2018) is consistent with this conclusion.

Our experiments have clarified the behavior of $CO_2/N_2$ mixtures under Venus temperature and pressure conditions and have provided essential information necessary to carry out future experiments. However, more work is needed. A future experiment should account for the sampling-induced mixing, as well as initial filling induced-turbulence or circulation, that needs to be taken into account.

**Situation near the surface of Venus.** Based on the experiments presented in this work, the composition gradient suggested by Lebonnois and Schubert (2017) in the deep atmosphere of Venus would be long-lived against molecular diffusion (timescales to mix a 7 km height layer are of the order of $10^{14}$ s), but would be affected over timescales controlled by turbulence or circulation (estimated to be of the order of $10^8$ s) (Cordier et al., 2019; Morellina and Bellan, 2019). Inserting a passive tracer in the IPSL Venus GCM (Lebonnois et al., 2018), with an initial composition that is horizontally uniform and reproduces the $N_2$ vertical gradient inferred in Lebonnois and Schubert (2017), simulations showed that the gradient is erased in the absence of any driving mechanism that would act against dynamical mixing. Within 3 Venus days of simulations (roughly one Earth year), the average surface amount of $N_2$ in the plains gets higher than 1%.

Therefore, to maintain the compositional gradient near the surface, sources and sinks of $CO_2$ and/or $N_2$ would be necessary, e.g. $CO_2$ injections accompanying volcanic activity. Some hypotheses are discussed in Cordier et al. (2019), in particular outgassing of $CO_2$ from the surface. Based on surface fluxes similar to the most active areas in the Yellowstone volcanic system, it seems possible to provide enough $CO_2$ to maintain the $N_2$ gradient against dynamical mixing. This outgassing might only be local, if the VeGa-2 probe descended over such an area, but the probability of such an event would depend on the surface of this active area. If this outgassing were global, such a maintained flux (estimated to be of the order of $10^{-3}$ mol $m^{-2}$ $s^{-1}$, Cordier et al., 2019) would increase the pressure at a rate of the order of 10 mbar/Ey, corresponding to one Venus atmosphere in less than 10000 Earth years.

The possibility of a $CO_2$ sink within the surface layer to compensate for this source, for example adsorption of $CO_2$ on basalt dust particles, is also difficult to defend.

When considering surface outgassing, we should also consider the possibility of a $SO_2$ source. This compound is heavier than $CO_2$ and a significant increase of $SO_2$ near the surface due to volcanism would also increase the mean molecular mass of the atmosphere. Considering a fixed and well-mixed $N_2$ content, a mole fraction of 2.8% of $SO_2$ is needed near the surface to get a mean molecular mass similar to pure $CO_2$ — which would be an extremely surprising coincidence. This means that $SO_2$ would decrease (linearly with altitude) from 2.8% near the surface to roughly 0.01% (100 ppm) at 7 km altitude. This seems difficult to maintain against dynamical mixing without a significant sink of $SO_2$ in this surface layer, hypothesis that is as difficult to defend as the others.

In addition to the pressure and temperature profile, and in the absence of direct measurement of composition, a probe that would be able to get an accurate measurement of the altitude could allow one to deduce the density profile through hydrostatic equilibrium, and, then, the amount of nitrogen through the equation of state. However, integrating the hydrostatic equilibrium based on a well-mixed $N_2$ profile, or on the $N_2$ profile inferred in Lebonnois and Schubert (2017), leads to altitude differences of around 40 m over 7 km, which may be too small to measure accurately from a landing probe. Therefore, in-situ composition measurements are mandatory to settle the question of the structure of the deep atmosphere of Venus.

### Data availability

Datasets related to this article are provided as supplementary files to this article.

### Acknowledgments

### Appendix A. Supplementary data

Supplementary material related to this article can be found online at https://doi.org/10.1016/j.icarus.2019.113550.

### References

Cordier, D., Bonhommeau, D., Port, S., Chevrier, V., Lebonnois, S., Garcia-Sanchez, F., 2019. The physical origin of the venus low atmosphere chemical gradient. Astrophys. J. 880, 82.

Cordier, D., Cornet, T., Barnes, J.W., MacKenzie, S.M., Le Bahers, T., Nna-Mvondo, D., Rannou, P., Ferreira, A.G., 2016. Structure of Titan's evaporites. Icarus 270, 41–56.

Duan, Z., Møller, N., Weare, J.H., 1996. A general equation of state for supercritical fluid mixtures and molecular dynamics simulation of mixture *PVTX* properties. Geochim. Cosmochim. Acta 60 (7), 1209–1216.

Duan, Z., Møller, N., Weare, J.H., 1992a. An equation of state for the CH4-CO2-H2O system: I. Pure systems from 0 to 1000°C and 0 to 8000 bar. Geochim. Cosmochim. Acta 56, 2605–2617.

Duan, Z., Møller, N., Weare, J.H., 1992b. Molecular dynamics simulation fo *PVT* properties of geological fluids and a general equation of state of nonpolar and weakly polar gases up to 2000 K and 20,000 bar. Geochim. Cosmochim. Acta 56, 3839–3845.

Gelman, B.G., Zolotukhin, V.G., Lamonov, N.I., Levchuk, B.V., Lipatov, A.N., Mukhin, L.M., Nenarokov, D.F., Rotin, V.A., Okhotnikov, B.P., 1979. Analysis of the chemical composition of the venus atmosphere on the venera 12 automatic interplanetary station with a gas chromatograph. Kosm. Issled. 17, 708–713.

Gnanaskandan, A., Bellan, J., 2018. Side-jet effects in high-pressure turbulent flows: Direct numerical simulation of nitrogen injected into carbon dioxide. J. Supercrit. Fluids 140, 165–181.

Gross, J., Sadowski, G., 2001. Perturbed-chain SAFT: An equation of state based on a perturbation theory for chain molecules. Ind. Eng. Chem. Res. 40 (4), 1244–1260.

Haney, E.D., Bliss, H., 1944. Compressibilities of nitrogen-carbon dioxyde mixtures. J. Supercrit. Fluids 36, 985–988.

Haynes, W.M. (Ed.), 2014. Diffusion in gases. In: CRC Handbook of Chemistry and Physics. CRC Press, Boca Raton, FL, ISBN: 9781482208689.

Hendry, D., Miller, A., Wilkinson, N., Wickramathilaka, M., Espanani, R., Jacoby, W., 2013. Exploration of high pressure equilibrium separations of nitrogen and carbon dioxide. J. $CO_2$ Util. 3–4, 37–43.

Hoffman, J.H., Hodges, R.R., Donahue, T.M., McElroy, M.M., 1980a. Composition of the Venus lower atmosphere from the Pioneer Venus mass spectrometer. J. Geophys. Res. 85, 7882–7890.

Hoffman, J.H., Oyama, V.I., von Zahn, U., 1980b. Measurement of the Venus lower atmosphere composition - A comparison of results. J. Geophys. Res. 85, 7871–7881.

Istomin, V.G., Grechnev, K.V., Kochnev, V.A., Ozerov, L.N., 1979. Composition of the lower venus atmosphere from mass spectrometer data.. Kosm. Issled. 17, 703–707.

Kliore, A.J., Moroz, V.I., Keating, G.M., 1985. The venus international reference atmosphere. Adv. Space Res. 5.

Lebonnois, S., Schubert, G., 2017. The deep atmosphere of Venus and the possible role of density-driven separation of $CO_2$ and $N_2$. Nat. Geosci. 10, 473–477.

Lebonnois, S., Schubert, G., Forget, F., Spiga, A., 2018. Planetary boundary layer and slope winds on venus. Icarus 314, 149–158.

Lee, B.I., Kesler, T.E., 1975. A generalized thermodynamic correlation based on th three paremeters corresponding states. AIChE J. 21, 510–527.

Linkin, V.M., Blamont, J.E., Lipatov, A.N., Devyatkin, S.I., D'yachkov, A.V., Ignatova, S.P., Kerzhanovich, V.V., Khlyustova, L.I., Malique, C., Sanotskil, Y.V., Shurupov, A.A., Stadnyk, B.I., Stolyarchuk, P.G., Terterashvili, A.V., 1986. Vertical thermal structure in the Venus atmosphere from provisional Vega 2 temperature and pressure data. Sov. Astron. Lett. 12, 40–42.

Lorenz, R.D., Crisp, D., Huber, L., 2018. Venus atmospheric structure and dynamics from the VEGA lander and balloons: New results and PDS archive. Icarus 305, 277–283.

Luspay-Kuti, A., Chevrier, V.F., Cordier, D., Rivera-Valentin, E.G., Singh, S., Wagner, A., Wasiak, F.C., 2015. Experimental constraints on the composition and dynamics of Titan's polar lakes. Earth Planet. Sci. Lett. 410, 75–83.

Morellina, S., Bellan, J., 2019. Characteristics of the venus lower atmosphere at different altitudes and chemical-species mixing properties computed using direct numerical simulation (in revision).

Mukhin, L.M., Gelman, B.G., Lamonov, N.I., Melnikov, V.V., Nenarokov, D.F., Okhotnikov, B.P., Rotin, V.A., Khokhlov, V.N., 1983. Gas-chromatographic analysis of the chemical composition of the Venus atmosphere aboard the automatic interplanetary stations Venera 13 and Venera 14. Kosm. Issled. 21, 225–230.

Oyama, V.I., Carle, G.C., Woeller, F., Pollack, J.B., 1980. Pioneer-Venus gas chromatography of the lower atmosphere of Venus. J. Geophys. Res. 85 (A13), 7891–7902.

Peplowski, P.N., Lawrence, D.J., 2016. Nitrogen content of Venus' upper atmosphere from the MESSENGER neutron spectrometer, in: Lunar and Planetary Science Conference, p. 1177.

Press, W., Teukolsky, S., Vetterling, W., Flannery, B., 1992. Numerical Recipes in Fortran, vol. 77. Cambridge University Press.

Seiff, A., Schofield, J.T., Kliore, A.J., et al., 1985. Model of the structure of the atmosphere of venus from surface to 100 km altitude. Adv. Space Res. 5 (11), 3–58.

Seiff, A., the VEGA Balloon Science Team, 1987. Further information on structure of the atmosphere of Venus derived from the VEGA Venus Balloon and Lander mission. Adv. Space Res. 7 (12), 323–328.

Span, R., Wagner, W., 1996. A new equation of state for carbon dioxide covering the fluid region from the triple-point temperature to 1100 k at pressures up to 800 MPa. J. Phys. Chem. Ref. Data 25, 1509–1596.

Tan, S.P., Kargel, J.S., Jennings, D.E., Mastrogiuseppe, M., Adidharma, H., Marion, G.M., 2015. Titan's liquids: Exotic behavior and its implications on global fluid circulation. Icarus 250, 64–75.

Tan, S.P., Kargel, J.S., Marion, G.M., 2013. Titan's atmosphere and surface liquid: New calculation using statistical associating fluid theory. Icarus 53–72.

von Zahn, U., Moroz, V., 1985. Composition of the venus atmosphere below 100 km altitude. Adv. Sp. Res. 5, 173–195.

Zasova, L.V., Moroz, V.I., Linkin, V.M., Khatuntsev, I.V., Maiorov, B.S., 2006. Structure of the venusian atmosphere from surface up to 100 km. Cosmic Res. 44, 364–383.